Arrangement Optimization of Phased Microphone Arrays Based on Deconvolution Algorithm

Xuyang Wang

School of Aeronautics and Astronautics,

Shanghai Jiao Tong University,

Shanghai, China

E-mail: wangxuyang1118@163.com

Wei Ma

School of Aeronautics and Astronautics,

Shanghai Jiao Tong University,

Shanghai, China

E-mail: mawei@sjtu.edu.cn

Abstract: Nowadays, phase microphone array is the main tool for acoustic source mapping. Previously, many scholars have studied and optimized the arrangement of microphone arrays based on beamforming algorithm. With the improvement of hardware and software performance and mapping accuracy requirements, deconvolution algorithm gradually shows its advantages. In this paper, the recognition capability of three different array types under deconvolution and beamforming algorithms are compared by dynamic range, spatial resolution and frequency span. The results show that under three different distribution of arrays, the deconvolution algorithm reduces the side-lobe effect, improves the dynamic range of acoustic source mapping, and improves the spatial resolution of the array. In terms of dynamic range, optimized spiral array have the best performance and circular array is similar to it with a satisfactory frequency range. However, the side-lobe effect of rectangular array can not be completely eliminated and the dynamic range is small. In terms of spatial resolution, the three arrays are equivalent, and circular array is slightly better than the optimized spiral array and the rectangular one. For frequency span, circular array also perform well. Therefore, in general, circular arrays can be considered as the preferred array arrangement for deconvolution algorithm.

Keywords: Microphone array; Beamforming; Deconvolution; Arrangement optimization.

1 Introduction

With the increasing application of microphone arrays in the field of acoustic measurement, growing research on this area are motivated. Beamforming algorithm is one of the most commonly used algorithms for acoustic source mapping, which is widely used in the identification and location of static and moving sound sources, including the acquisition of sound source information for aircraft, high-speed trains and vehicles [1]. The advantage of this algorithm is its simplicity and directness, short operation time, high efficiency, and low requirement for computer hardware [2]. However, due to the defect of principle, the number of side-lobes of constant sound source in the source reconstruction image acquired by beamforming algorithm is large, and it is not much different from the real sound source, so it can not be distinguished and then affect the results [3, 4, 5]. The spatial resolution of traditional beamforming algorithm is poor as well, and the location accuracy of complex sound sources is unsatisfactory for the requirement of today. The deconvolution algorithm is an advanced algorithm developed to overcome the disadvantages of beamforming. Brooks and Humphreys [6] proposed DAMAS, as an optimized deconvolution algorithm for source recognition and location. The principle is as follows: Firstly, a rough source reconstruction map is obtained by using the traditional beamforming algorithm; Then obtained the convolution relation between rough beamforming result, the point spread function(PSF) and the real sound source distribution. Finally, deconvolution through iteration and then reconstruct accurate reconstruction map. Because of eliminating the influence of non-ideal point spread function, deconvolution algorithm effectively suppresses the level of side-lobes of sound source, reduces the error of source identification and location, and significantly improves the spatial resolution and dynamic

range of microphone arrays. Unfortunately, the computational efficiency of DAMAS is poor and it takes a lot of time to solve the real sound source distribution iteratively. Thus, the deconvolution algorithm is not widely used. However, with the proposal of various optimization methods, including DAMAS2 [7], NNLS [8, 9], and advanced methods of compression computational grid [10, 11], etc., the disadvantage of deconvolution algorithm is lessened. Meanwhile, with the improvement of hardware and software performance and mapping accuracy requirements, deconvolution algorithm shows its advantages.

When designing a microphone array, it is necessary to synthesize various factors affecting the performance of the array, including the geometric and experimental parameters of the array. Among these factors, array structure is the core of array performance. The arrangement optimization of microphone arrays has been carried out for a long time. In 1975, NASA researchers Soderman and Nobel [12] designed the simplest one-dimensional linear uniform microphone array based on the principle of delay-and-sum algorithm for noise source measurement in wind tunnels. At the same time, Billingsley and Kinns [13] also constructed a one-dimensional linear array to locate the sound source of a full-scale jet engine. Michel et al. [14] measured the noise emissions of Tornado fighters in 1997 using a one-dimensional uniform linear array of twenty-nine microphones. With the continuous development of microphone array technology, array layout has gradually evolved from one-dimensional linear array to two-dimensional planar array, and the number of microphones used in array is increasing. Rectangular and circular arrays [15] are gradually proposed and put into use [16, 17]. In 2002, Dougherty and Underbrink [18] designed dobby helical arrays to measure noise at larger frequencies. However, as the traditional beamforming algorithm has been widely used in the field of sound source identification and location, so far almost all the optimization designs of microphone arrays are based on this algorithm. At present, there is little research on array optimization based on deconvolution algorithm. With ever higher accuracy requirements, deconvolution algorithm is expected to replace traditional beamforming algorithm as the most common source localization algorithm in the next future, and the research of array optimization based on deconvolution algorithm is imminent.

In this paper, three different common distribution of microphone arrays are simulated under both beamforming and deconvolution algorithms. The goal of such simulations is to find how much advantages does the deconvolution algorithm have over the beamforming algorithm and which distribution of arrays is the optimal under deconvolution algorithm. The comparison is focused on dynamic range and spatial resolution.

Fig. 1 is a simplified schematic of dynamic range and spatial. Dynamic range and spatial resolution are the most significant characters to evaluate microphone array. In the map of microphone array response, the main beam is called the main lobe, while the other small-amplitude beams are called the side-lobes. The dynamic range of the array is defined as the difference of the peak value of the side-lobes relative to the main lobe, which represents the ability of the microphone array to identify the sound source. Sound sources whose intensity is lower than the side-lobes can not be identified. The larger the dynamic range is, the wider the range of sound sources that microphone arrays can recognize, and the more accurate the result of sound source mapping is.

Spatial resolution is defined as the smallest distance between two sound sources in space that can be distinguished by an array. High spatial resolution also means high accuracy of sound source identification and location. In order to describe spatial resolution more accurately, the array beam width (BW) is used as a measure parameter. Spatial resolution can be defined as the main lobe width of 3dB below the peak value in the array response map [19].

In addition, in order to ensure the wide applicability of the microphone arrays, the frequency span is another significant object of investigation. The wider the range of microphone arrays, the wider the scope of application.

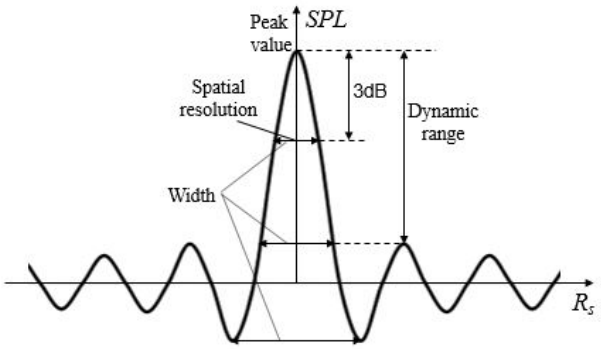

Fig. 1. Simplified schematic of dynamic range and spatial

2 Design of Microphone Arrays

In this section, the microphone distributions used in the simulations are designed according to the principle of microphone array designing. And the main parameters of the arrays are compared.

2.1 Principle of Design

Certain principles must be followed when designing a microphone array. The basic principle of the design is to improve the spatial resolution and dynamic range of the array according to the actual application requirements, while avoiding the appearance of sound source side-lobes. How to obtain the best performance microphone array to meet the design requirements under the control of production cost and installation difficulty is the focus and difficulty of optimizing the microphone array design.

The number of elements and the array aperture are the core factors that determine the complexity of microphone arrays [20]. The more microphone array elements, the more complex the installation and layout [21]. The array aperture

size determines the size of the whole device. The larger the array aperture, the larger the installation space required. In addition, the number of microphones directly affects the gain of microphone arrays. The larger the gain, the better the improvement level of signal-to-noise ratio of microphone arrays. The array element spacing refers to the distance between the two nearest microphones in the microphone array, which directly affects the sound source mapping accuracy. When the spacing of the array elements is increased, the beam width becomes smaller and the positioning accuracy is improved. When a uniform array is used for sound source identification and localization, grating lobes may appear in the sound source map. The appearance of the grating-lobes can cause spatial aliasing effects and affect the array test results. The appearance of the grating- lobes is affected by the distribution layout, the spacing of the elements, the frequency of the sound source, and the beam pointing, etc. In order to prevent the occurrence of the grating-lobes, there is an upper limit on the distance between two adjacent microphones of the uniform array, that is, the spacing of the array elements cannot be greater than half a wavelength, that is, the Nyquist sampling criterion is satisfied:

$$\mathrm{d}_e \leq \frac{\lambda}{2} = \frac{c_0}{2f} \tag{1}$$

Where d_e is the distance between the nearest two is array elements, λ is the wavelength is sound source, c_0 is sound speed and f is the frequency of sound source.

2.2 Distribution Arrangement

In general industrial production, the distributions of microphone arrays are generally divided into circular, rectangular and spiral, etc. Thus, this paper also adopt these three distributions to study. According to the above design principles, this paper design a circular equidistant distribution array, a rectangular equidistant distribution array and an optimized spiral distribution array, as shown in Fig.2. The circular equidistant distribution array place 64 microphone sensors on a circumference with a diameter of 1m equidistantly. The rectangular equidistant distribution array place sensors evenly on the nodes of 7 x 7 square grid in a square with side length of 1m. The structures of these two kinds of array are simple, which greatly reduces the complexity of microphone array system. The so called optimized spiral distribution array is put forward by Underbrink[18, 22], the sensors are placed equidistantly on a logarithmic spiral, then use the symmetric character to get multiple spirals. The polar coordinate equation of the logarithmic spiral [23] is:

$$\mathrm{r}(\theta) = r_0 \exp[\cot(\upsilon)\theta] \tag{2}$$

Where r is the distance between the origin and the point on the spiral, θ is the polar angle in radians, r_0 is the distance between the origin and the starting point of the spiral, and υ is the helix angle. In this paper, the helix angle is $\pi/4$ and r_0 is 0.05m. The number of spiral arms is nine, and seven sensors are placed on each arms. The radius of the circle formed by the outermost sensors is 0.5m.

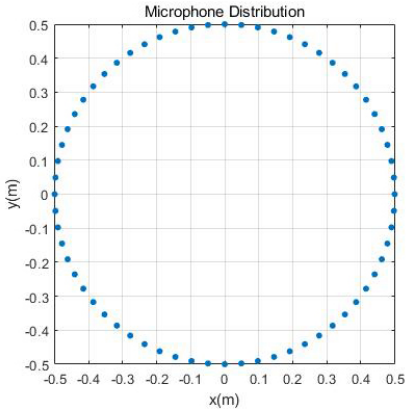

(a)

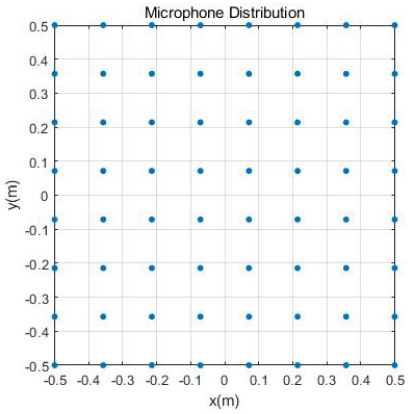

(b)

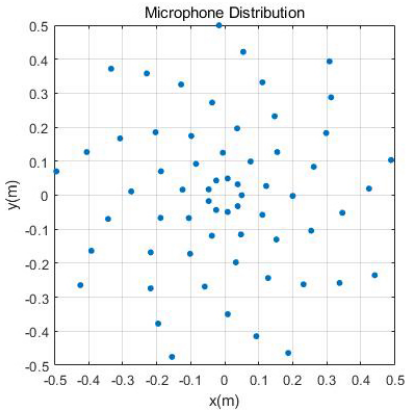

(c)

Fig. 2. Arrays Distribution. (a) Circular equidistant distribution array. (b) Rectangular equidistant distribution array. (c) Optimized spiral distribution array

Table.1 show the comparison of the arrays parameters. Their array aperture size is the same. The number of the optimized spiral distribution array is one less than the circular equidistant distribution array and the rectangular equidistant distribution array, but the effect is very small and can be approximated as equal.

Table.1 Arrays parameter comparison

Arrangement Distribution	Number of elements	Array size(m)	d_e(m)
Circular equidistant	64	1	0.049
Rectangular equidistant	64	1	0.125
Optimized spiral	63	1	0.035

3 Results and Discussion

In this section, simulation experiments are carried out on Matlab to study base on the basic theory of arithmetic and the theory of array measurement. The dynamic range and spatial resolution of different arrays are compared, and the frequency range of the arrays is compared by the performance of the array under different frequency sound sources. The general experimental conditions are shown in Fig. 3. The array plane is parallel to the sound source plane. The plane distance z_0 is 5m, the flare angle α is 60°. Sound source plane is divided into grids of 30 x 30. When calculating based on deconvolution algorithm, the maximum number of iterations is 2000. The sound speed is defined as a fixed value, 340 m/c. The sampling frequency of microphone elements is 44.1 kHz. The reference sound source frequency is defined as 2000Hz, as it is common frequency of noise during the take-off and landing of the plane [24].

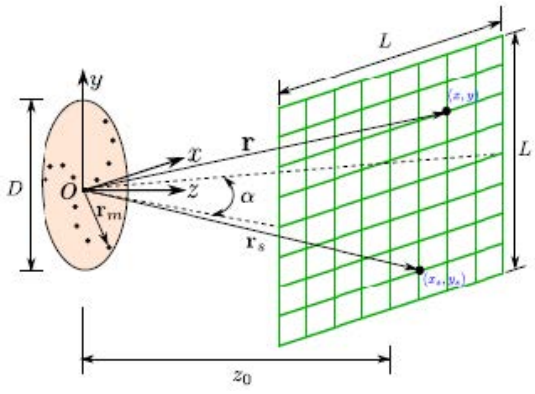

Fig. 3. Sketch of array plane and sound source plane [11].

3.1 Dynamic Range

In this part, seven point acoustic sources are used as the signals. These seven point sources are placed at coordinates (0, 0), (1, 1.732), (-1, 1.732), (-2, 0), (-1, -1.732), (1, 1.732) and (2, 0), they are at the centre of a regular hexagon and its corners, as shown in Fig. 4. Their sound pressure levels(SPL) are defined as 0dB, -2dB, -4dB, -6dB, -8dB, -10dB, -12dB, respectively. They have a same frequency, 2000Hz.

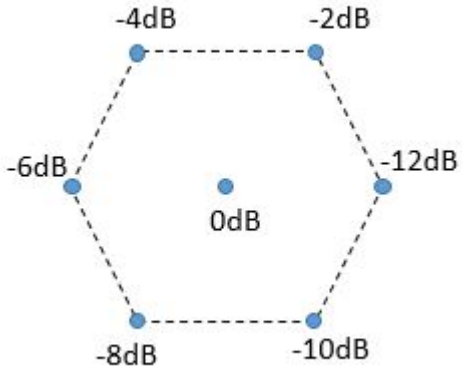

Fig. 4. Sketch of arrangement of sound source signals.

The corresponding identification maps are shown in Fig.5. Fig. 5a is the beamforming map of circular equidistant distribution array. It has a high level of side-lobes and a significant spatial aliasing effect. It is hard to identify the information of sound source by this map. Fig. 5c and Fig. 5e show the beamforming maps of rectangular equidistant distribution array and optimized spiral distribution array. Under beamforming algorithm, the rectangular array generally orderly identifies the sound sources. In the meanwhile, however, the side-lobes still exist, it will interfere with the correct acquisition of sound source information. The dynamic range of the rectangular array is about 8dB. The optimized spiral distribution array well mapped the sound source without any side-lobes. Its dynamic range is above 12dB. Fig. 5b, Fig. 5d and Fig. 5f show the DAMAS maps of corresponding arrays, respectively. Compared with the results of beamforming algorithm, the beamwidths of DAMAS maps have obvious reduction. In more detail, the circular equidistant array and the optimized spiral array are similar, they well mapped all the sound source points except for the -12dB one, with negligible side-lobes near the main-lobes of high amplitude. Both of their dynamic ranges are about 12dB. The rectangular equidistant distribution array lose the -12dB sound source point, and there are still obvious side-lobes at the edge of the map. In this aspect, it works worse than the other two.

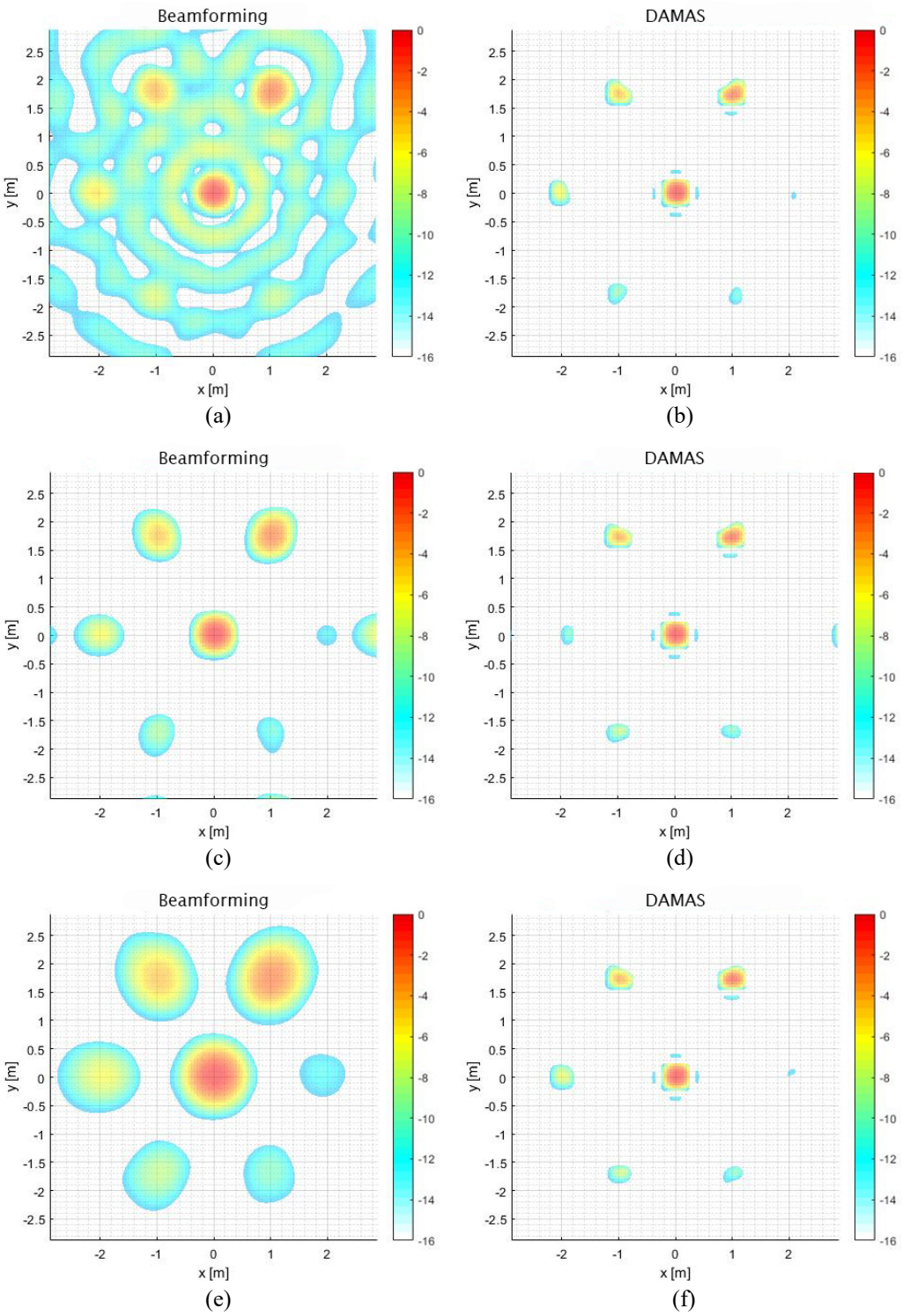

Fig. 5. Identification map. (a) Beamforming map of circular equidistant distribution array. (b) DAMAS map of circular equidistant distribution array. (c) Beamforming map of rectangular equidistant distribution array. (d) DAMAS map of rectangular equidistant distribution array. (e) Beamforming map of optimized spiral distribution array. (f) DAMAS map of optimized spiral distribution array.

3.2 Spatial Resolution

In this simulation, nine point sources are placed at (-1.2, 1.2), (0, 1.2), (1.2, 1.2), (-1.2, 0), (0, 0), (1.2, 0), (-1.2, -1.2), (0, -1.2), (1.2, -1.2) with a same frequency of 2000Hz. The SPL are all defined as 0dB. since that spatial resolution can be defined as the main lobe width of 3dB below the peak value in the array response map [19], the response maps are set to display only the -3dB to 0dB portion. The Average diameters of the main lobes are defined as the beamwidths. The response maps are shown in Fig. 6. Fig.6a shows that under beamforming algorithm, circular equidistant distribution array still exist side-lobes even when the pre-set

dynamic range is only 3dB. The beamforming maps of rectangular equidistant distribution array and optimized spiral distribution array are shown in Fig.6c and Fig.6e. Their spatial resolution is 0.58m and 0.90m respectively, without side-lobes. Fig. 6b, Fig. 6d, Fig. 6f show the corresponding maps of the three arrays based on deconvolution algorithm. It is simple to see that the spatial resolution of the three arrays is significantly improved based on the deconvolution algorithm, reached 0.30m, 0.32m and 0.31m respectively. Thus, these three array have similar spatial resolution under DAMAS.

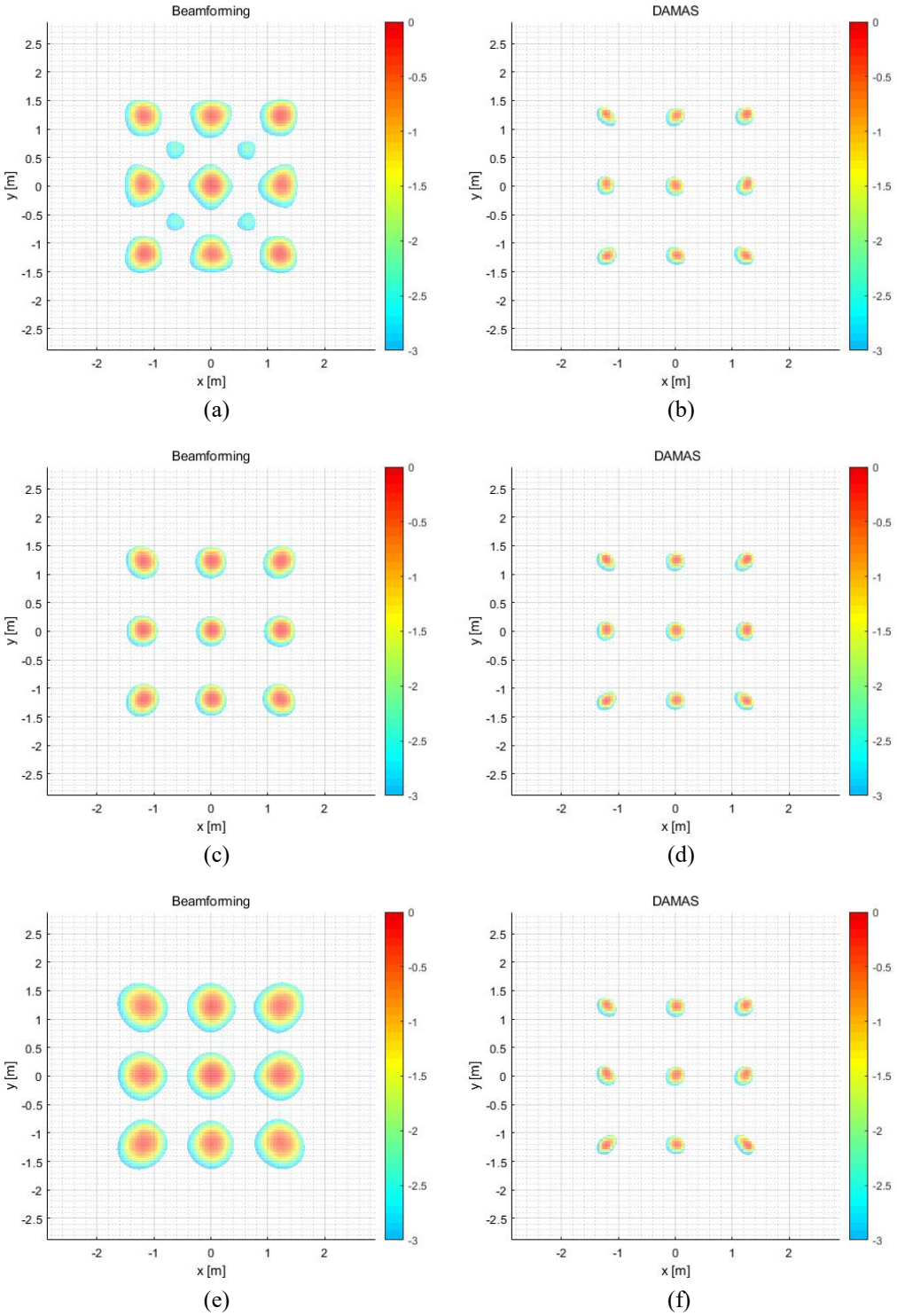

Fig. 6. Identification map for beamwidths. (a) Beamforming map of circular equidistant distribution array. (b) DAMAS map of circular equidistant distribution array. (c) Beamforming map of rectangular equidistant distribution array. (d) DAMAS map of rectangular equidistant distribution array. (e) Beamforming map of optimized spiral distribution array. (f) DAMAS map of optimized spiral distribution array.

3.3 Frequency Span

In addition to dynamic range and spatial resolution, frequency span is also a significant feature. If the former two means the accuracy of microphone arrays, then the frequency span represents the application scope of microphone arrays. In this part, the performance of the arrays on different frequencies are compared based on DAMAS. The location and pressure levels of the sound signals are the same as used in the first part as shown in fig. 4. The frequencies tested are 500Hz, 1000Hz, 2000Hz, 4000Hz and 8000Hz. As it is already proved that DAMAS has a superior accuracy, here the simulation based on beamforming is not attached.

The identification results of microphone arrays under different frequency sound sources are shown in Fig. 7. When the source frequency is 500 Hz, the circular equidistant distribution array and the rectangular equidistant distribution array have better performance, while the optimized spiral distribution array has side-lobes and the main lobes are large. As the frequency of sound source increases to 4000Hz, circular array and helical array still perform well, only with a slight decrease of dynamic range. However, the spatial aliasing effect of rectangular array has gradually occurred since 2000 Hz, it is already quite serious when the frequency reaches 4000Hz. When the source frequency reaches 8000Hz, both circular equidistant distribution array and the rectangular one have serious spatial aliasing effect, the optimized spiral distribution array still work well, with slight side-lobes.

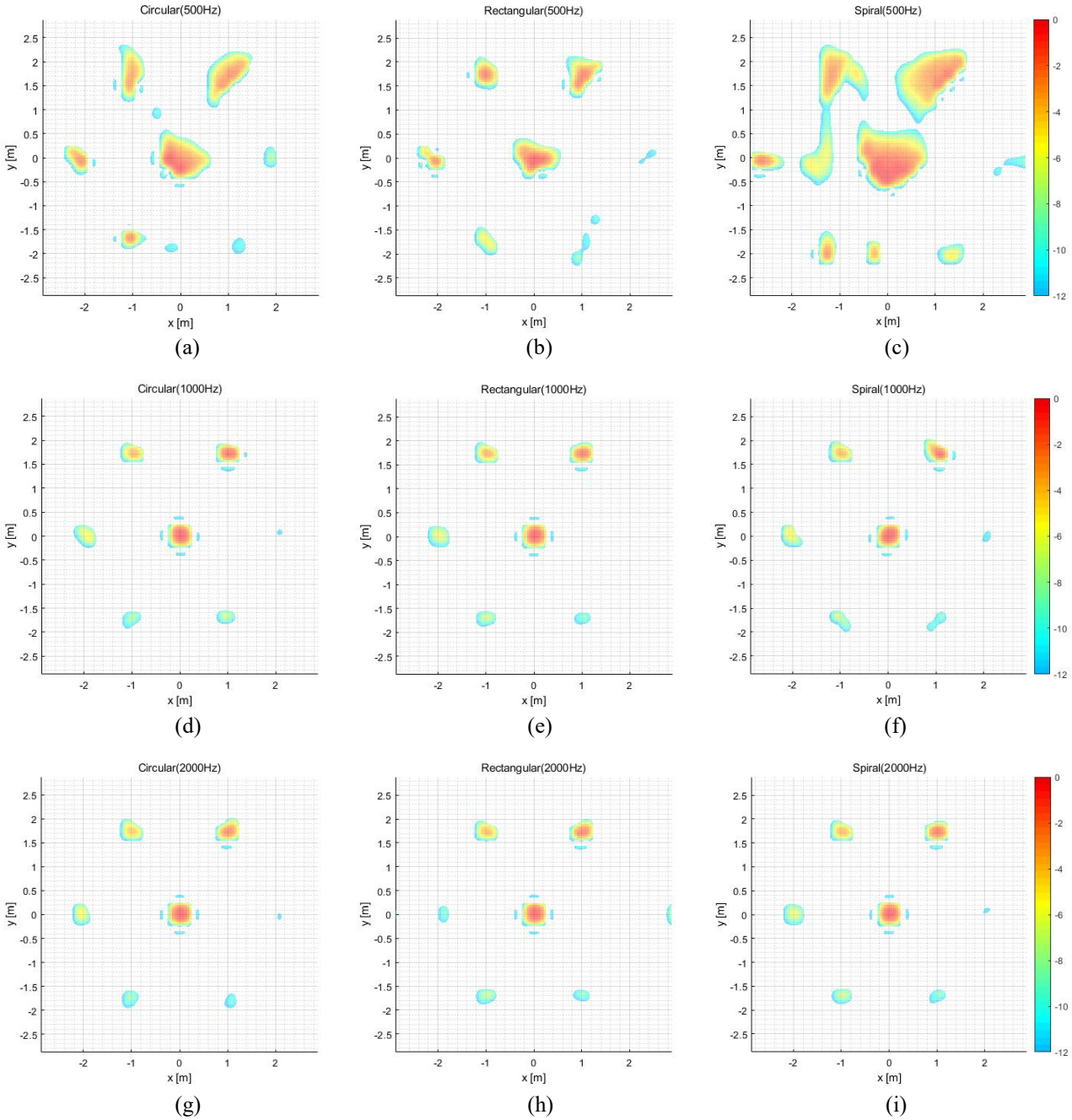

(a) (b) (c)

(d) (e) (f)

(g) (h) (i)

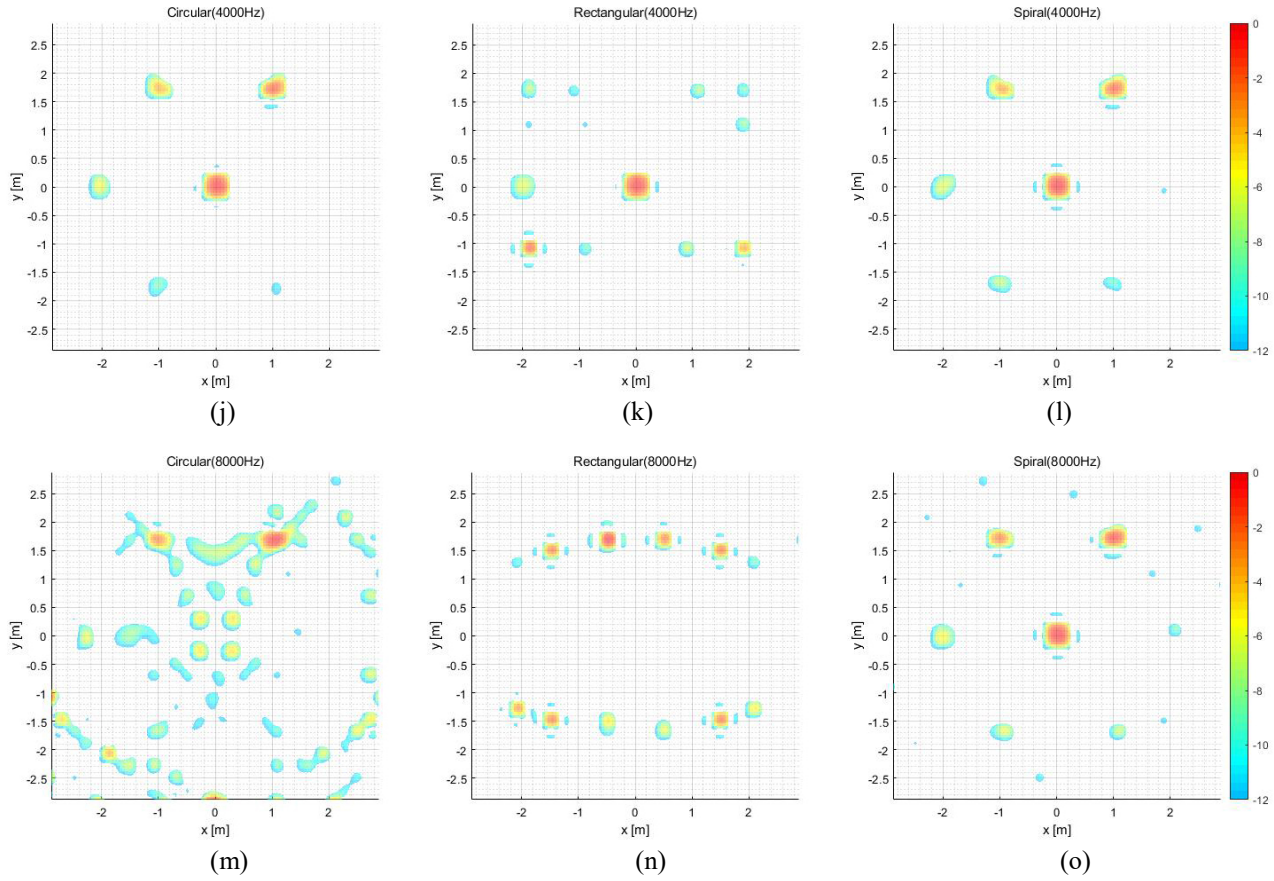

Fig. 7. Identification map for different frequencies under DAMAS. (a) Map of circular array (500Hz). (b) Map of rectangular array (500Hz). (c) Map of spiral array (500Hz). (d) Map of circular array (1000Hz). (e) Map of rectangular array (1000Hz). (f) Map of spiral array (1000Hz). (g) Map of circular array (2000Hz). (h) Map of rectangular array (2000Hz). (i) Map of spiral array (2000Hz). (j) Map of circular array (4000Hz). (k) Map of rectangular array (4000Hz). (l) Map of spiral array (4000Hz). (m) Map of circular array (8000Hz). (n) Map of rectangular array (8000Hz). (0) Map of spiral array (8000Hz).

4 Conclusions

This paper design and compare three distributions of microphone arrays. The comparison show that deconvolution Algorithm does have great superiorities over conventional beamforming algorithms. Under the deconvolution algorithm, the circular equidistant distribution array and the optimized spiral distribution array have better features than the rectangular one on dynamic range. More specifically, the performance of circular one in low frequency band is better than that of the optimized spiral distribution arrays, while the latter have some advantages in high frequency band. Nevertheless, the optimum operating frequency band size of the two systems is similar and their overlap range is large. When the deconvolution algorithm is widely applied on microphone arrays, spiral arrays are no longer as advantageous as under beamforming algorithm. Thus, considering the manufacturing cost and installation difficulty of microphone array, circular equidistant distribution array can replace spiral array as the preferred microphone array based on deconvolution algorithm.

Reference

[1] Valin, J.M., Michaud, F. and Rouat, J., 2007. Robust localization and tracking of simultaneous moving sound sources using beamforming and particle filtering. Robotics and Autonomous Systems, 55(3), pp.216-228.

[2] Van Veen, B.D. and Buckley, K.M., 1988. Beamforming: A versatile approach to spatial filtering. IEEE assp magazine, 5(2), pp.4-24.

[3] Michel, U., 2006, November. History of acoustic beamforming. In Berlin Beamforming Conference, Berlin, Germany, Nov (pp. 21-22).

[4] Malgoezar, A., Snellen, M., Sijtsma, P. and Simons, D., 2016, February. Improving beamforming by optimization of acoustic array microphone positions. In Proceedings of the 6th Berlin Beamforming Conference (p. 5).

[5] Christensen, J.J. and Hald, J., 2004. Technical review beamforming. Bruël & Kjær, 1.

[6] Brooks, T.F. and Humphreys, W.M., 2006. A deconvolution approach for the mapping of acoustic sources (DAMAS) determined from phased microphone arrays. Journal of Sound and Vibration, 294(4-5), pp.856-879.

[7] R.P. Dougherty, Extension of DAMAS and benefits and limitations of deconvolution in beamforming, AIAA 2005e2961 (2005).

[8] Lawson, C.L. and Hanson, R.J., 1995. Solving least squares problems (Vol. 15). Siam.

[9] Ehrenfried, K. and Koop, L., 2007. Comparison of iterative deconvolution algorithms for the mapping of acoustic sources. AIAA journal, 45(7), pp.1584-1595.
[10] Ma, W. and Liu, X., 2017. Improving the efficiency of DAMAS for sound source localization via wavelet compression computational grid. Journal of Sound and Vibration, 395, pp.341-353.
[11] Ma, W. and Liu, X., 2017. DAMAS with compression computational grid for acoustic source mapping. Journal of Sound and Vibration, 410, pp.473-484.
[12] Soderman, P.T. and Noble, S.C., 1975. Directional microphone array for acoustic studies of wind tunnel models. Journal of Aircraft, 12(3), pp.168-173.
[13] Billingsley, J. and Kinns, R., 1976. The acoustic telescope. Journal of Sound and Vibration, 48(4), pp.485-510.
[14] Michel, U., Barsikow, B., Haverich, B., Schüttpelz, M., Michel, U., Barsikow, B., Haverich, B. and Schuettpelz, M., 1997, May. Investigation of airframe and jet noise in high-speed flight with a microphone array. In 3rd AIAA/CEAS Aeroacoustics Conference (p. 1596).
[15] Dougherty, R.P., Scharpf, D.F. and Underbrink, J.R., 1995. Test Report Boeing/NASA Ames Flap-Edge Noise Test: Phased-Array Development. NASA CDTR, pp.21-000.
[16] Van, H.T., Bell, K. and Tiany, Z., 2013. Detection Estimation and Modulation Theory. In Detection, Estimation, and Filtering Theory. Wiley & Sons, Inc., pp.293-303.
[17] Baptiste, P.J. and Jules, M.A., 1926. Telescope of the right-angled type with fixed eyepiece and movable objective, chiefly applicable to the observation of aerial objects. U.S. Patent 1,607,688.
http://www.freepatentsonline.com/1607688.html
[18] Underbrink, J.R., 2002. Aeroacoustic phased array testing in low speed wind tunnels. In Aeroacoustic measurements (pp. 98-217). Springer, Berlin, Heidelberg.
[19] Mueller, T.J. and Prasad, M.G., 2003. Aeroacoustic Measurements. Applied Mechanics Reviews, 56, p.B66.
[20] Steinberg, B.D., 1976. Principles of aperture and array system design: Including random and adaptive arrays. New York, Wiley-Interscience, 1976. 374 p, pp.189-190
[21] Pirz, F., 1979. Design of a wideband, constant beamwidth, array microphone for use in the near field. Bell System Technical Journal, 58(8), pp.1839-1850.
[22] Underbrink, J.R., 1996. Array design for non-intrusive measurement of noise sources. Proc. Noise-Con 96.
[23] Eugene, A. and Baumeister, T., 1996. Marks' Standard Handbook for Mechanical Engineers--Revised by a Staff of Specialists. McGraw-Hill.
[24] MICHAEL, J., "Sound camera'silences a mystery", Boeing Frontiers